JOURNAL OF GUIDANCE, CONTROL, AND DYNAMICS
Vol. 17, No. 4, July–August 1994

Onboard Stationkeeping of Geosynchronous Satellites Using a Global Positioning System Receiver

C. C. Chao* and H. Bernstein†
The Aerospace Corporation, El Segundo, California, 90009

Many space missions are considering the use of a Global Positioning System (GPS) receiver as a means of onboard ephemeris determination due to its portability, accuracy, and low cost. A feasibility study of onboard stationkeeping using a GPS receiver has been performed. This paper describes three strategies for onboard stationkeeping utilizing onboard GPS measurements. Algorithms are developed and accuracies of orbit control are assessed based on proposed strategies and covariance analysis. Although this study is focused on the application to geosynchronous satellites, the same technique applies to other missions with circular orbits. The innovative strategy of formation keeping a satellite with a fictitious satellite whose ephemeris is predetermined can significantly improve the long-term prediction accuracy without ground support. Results of simulations show that the maximum deviations from a predetermined ephemeris range from less than 0.1 km to 0.3 km dependent on onboard hardware/software options.

Introduction

THE Global Positioning System (GPS) receiver has become an attractive means of onboard autonomous ephemeris determination due to its portability (15 lb), accuracy (20–100m) and low cost ($100,000–300,000). The cost estimate includes a space-qualified receiver with antenna design. The actual cost should come down as the number of users increases. For low-attitude orbits, instant position determination is possible due to good visibility to GPS satellites. However, for geosynchronous satellites, the visibility is limited to a small conical annulus formed by the main beam skirt outside the GPS-Earth cone. Ananda and Jorgensen[1] have indicated that, with a GPS receiver and a 10-turn helical antenna on board the spacecraft, the ephemeris of a geostationary satellite can be determined autonomously or semi-autonomously with a sequential filter. A recent paper by Wu et al.[2] discussed the GPS-based tracking of Earth satellites from low to geosynchronous orbits. The concept of onboard stationkeeping using a GPS receiver has not previously been explored. This concept requires an onboard processor to monitor and periodically issue commands for stationkeeping when the ephemeris deviations from a reference, determined by GPS measurements, exceed the tolerance. For missions requiring tight orbit control, the concept of onboard stationkeeping using onboard GPS measurements has several advantages. These advantages are 1) the significant cost savings for greatly reduced ground operations, 2) the high-accuracy, long-term ephemeris supplied to the users several months in advance for improved mission performance, and 3) less dependence on overseas stations.

This study is focused on the application of this concept to geosynchronous satellites. The visibility history of GPS satellites is examined for 24-h orbits with low and high inclinations. The accuracy of position determination based on the visibility history and a sequential filter is assessed. Then the onboard GPS-determined ephemeris with the assessed accuracy is applied to onboard stationkeeping through three proposed control strategies. These strategies can be used for onboard orbit control for other circular or near-circular orbits at different altitudes. Control strategies for noncircular orbits were not considered.

Presented as Paper 92-4655 at the AIAA/AAS Astrodynamics Conference, Hilton Head, SC, Aug. 10–12, 1992; received Oct. 31, 1992; revision received June 28, 1993; accepted for publication July 29, 1993.

*Manager, Orbit Dynamics Section, Systems Engineering Division, P.O. Box 92957, M4/946. Member AIAA.

†Manager, Satellite Navigation Section, Systems Engineering Division, P. O. Box 92957, M3/952.

GPS Visibility to Geosynchronous Satellites

It was assumed that the GPS L1 and L2 carrier signals can be received only when the geosynchronous satellite is within a conical annulus formed by the downward pointing main beam skirt of the GPS primary antenna as shown in Fig. 1. At the GPS satellite, the half-cone angle covering the Earth's shadow is about 14 deg. The total half-cone angle to the outer edge of the conical annulus was 21 deg.

Because of this visibility geometry, four GPS satellites are never simultaneously observed as is the case for Earth surface and low-orbiting satellite GPS users. At any measurement time, there is not enough information to form four independent equations to solve explicitly for four unknowns (three components of position plus the receiver clock offset from GPS time). A sequential filter capable of predicting state vector parameters to the next measurement time provides an a priori (premeasurement) estimate of navigation parameters and receiver clock offset, allowing even one GPS measurement to improve on this a priori. This situation explains why navigation error is sensitive to the quality of the GPS receiver clock. Since the clock offset cannot be explicitly solved for, there is greater sensitivity to its stability.

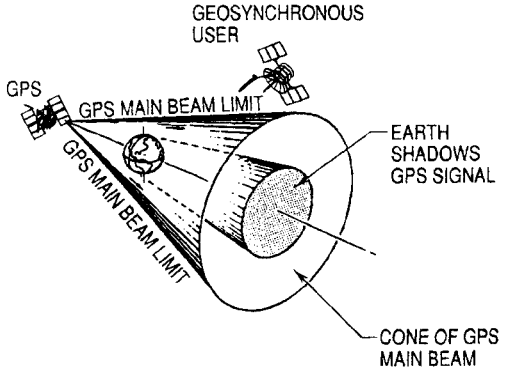

Fig. 1 Geosynchronous user-GPS tracking geometry.

Covariance Analysis of Onboard GPS Ephemeris Determination

The navigation error analysis modeled a sequential filter whose state vector consisted of three position components, three velocity components, two clock terms (phase and frequency), and an in-track ΔV impulse. Errors in unmodeled forces (Earth gravity, solar radiation, momentum dumps, commanded thrusts) were taken into account. It turns out that the satellite position estimation accuracy is relatively insensitive to force model errors. Measurements are taken every 12 min. A few measurement gaps exist that do not exceed 2 h. The ephemeris prediction error, caused by force model errors, over these short periods of time (before a GPS measurement is available to make a correction) is very small, thus accounting for this relative insensitivity. For this reason, the modeling of gravity and solar radiation pressure was simplified and very conservative. These modeling errors are 1) 1.0×10^{-8} m/s^2, unmodeled solar pressure acceleration along the sun line; 2) 1.0×10^{-9} m/s^2, unmodeled solar pressure acceleration perpendicular to the sun line; 3) 0.35×10^{-7} m/s^2, acceleration error due to gravity constant (very conservative); and 4) 0.44×10^{-7} m/s^2, 1.8×10^{-10} m/s^2, and 1.6×10^{-9} m/s^2, radial, in-track, and cross-track acceleration errors due to gravity harmonics. GPS receiver clock phase and frequency noise as well as measurement errors were modeled.

Figure 2 displays the measurements obtained during a 24-h period and is to be interpreted as follows: Dots are drawn at the 12-min measurement interval that was used. The zero value on the ordinate shows those measurement times when there were no GPS measurements. The positive numbers ranging from 1 to 21 are index numbers for an optimized constellation (see Table 1) and show the times when a measurement was made to these satellites. The negative numbers show the total number of GPS satellites to which measurements were made at the time points. The visibility pattern repeats daily with minor variations for a given initial relative geometry. Results show that the visibility pattern varies slightly for different initial geometry and inclination of geosynchronous orbit.

Navigation error analyses were performed for two receiver clocks of different quality. These were an atomic reference having the same order of stability (1×10^{-13}) as that on the GPS satellites and a precision crystal clock (1×10^{-11} stability). Also, the analysis included variations in measurement type. In one case only pseudorange (PR) measurements were used. For an authorized user able to remove the selective availability corruption, the ranging error model included a 6-m, 1σ error due to GPS satellite ephemeris and clock broadcast message errors. The total RSS 1σ ranging error due to GPS satellite and receiver was 7 m, consisting of bias and random components. An accumulated delta pseudorange measurement with a random 1σ error of 1 cm in addition to the pseudorange measurement

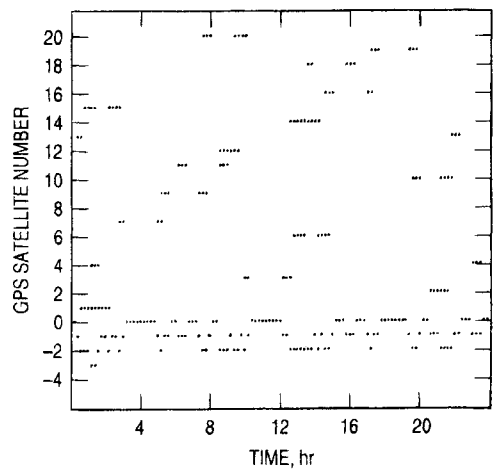

Fig. 2 GPS visibility to geosynchronous satellite.

Table 1 GPS trajectory initial conditions

Satellite index	Right ascension, deg	Mean anomaly, deg
1	30.0	137.0
2	30.0	257.0
3	30.0	17.0
5	90.0	177.0
6	90.0	297.0
7	90.0	57.0
8	150.0	217.0
9	150.0	337.0
10	150.0	97.0
12	210.0	257.0
13	210.0	17.0
14	210.0	137.0
15	270.0	297.0
16	270.0	57.0
17	270.0	177.0
19	330.0	337.0
20	330.0	97.0
21	330.0	217.0
4	30.0	167.0
11	150.0	307.0
18	270.0	87.0

Eccentricity = 0
Semimajor axis = 26559800.0 m
Inclination = 55 deg
Argument of perigee = 0.0 deg

was also examined in a second case. Results are also presented for an unauthorized user having a (1σ) 36-m ranging error. A real data analysis by Malys and Holm[3] showed more optimistic results for both authorized and unauthorized users.

Figures 3 and 4 display estimation accuracy of navigation and clock parameters using PR measurements only, for the two clock models, for an authorized user. Figures 3a and 3b show the accuracy with which the onboard clock can be synchronized to GPS time. Figures 3c and 3d show RMS position accuracy. The disturbance starting at about 8 h is due to the application of a stationkeeping thrust (modeled as a velocity impulse) at this time. Some of the choppiness in the plots is due to measurement gaps. Figures 4a–4d display position and velocity 1σ component errors in radial, in-track, and cross-track coordinate systems. The impulsive stationkeeeping velocity impulse uncertainty was modeled to occur in the in-track direction. Figure 4e displays the ability of the estimation algorithm to estimate the applied velocity impulse. The initial 1σ uncertainty of about 0.007 m/s can be reduced significantly.

The addition of the accumulated delta pseudorange measurement with measurements occurring every 1.5 min may lead to a significant improvement in navigation accuracy. Average rms position error using the atomic standard was below 10 m. However, this new data type needs further investigation, and it was not included in this analysis. The results presented are for low-inclination orbits (i = 0.5 deg). High-inclination orbits (i = 70 deg) showed slight improvement in navigation accuracy probably due to slightly better visibility.

Results for the unauthorized user are shown in Figs. 5a–5d. Figure 5a shows the rms position error. Figures 5b and 5c show the 1σ component position and velocity errors. Figure 5d shows the accuracy with which the onboard clock can be synchronized to GPS time. Note that the clock offset estimate is still converging.

Strategies of Onboard Stationkeeping

Three stationkeeping strategies for onboard orbit control are considered in this analysis. The first two strategies are designed for controlling the in-track motion or geographic longitude of a satellite, whereas the last strategy controls the satellite motion in three dimensions (in track, radial, and cross track). The accuracy of onboard GPS navigation is based on the covariance analysis results described in the previous section with position and velocity errors shown in Figs. 3c–4d and Table 2. Figures

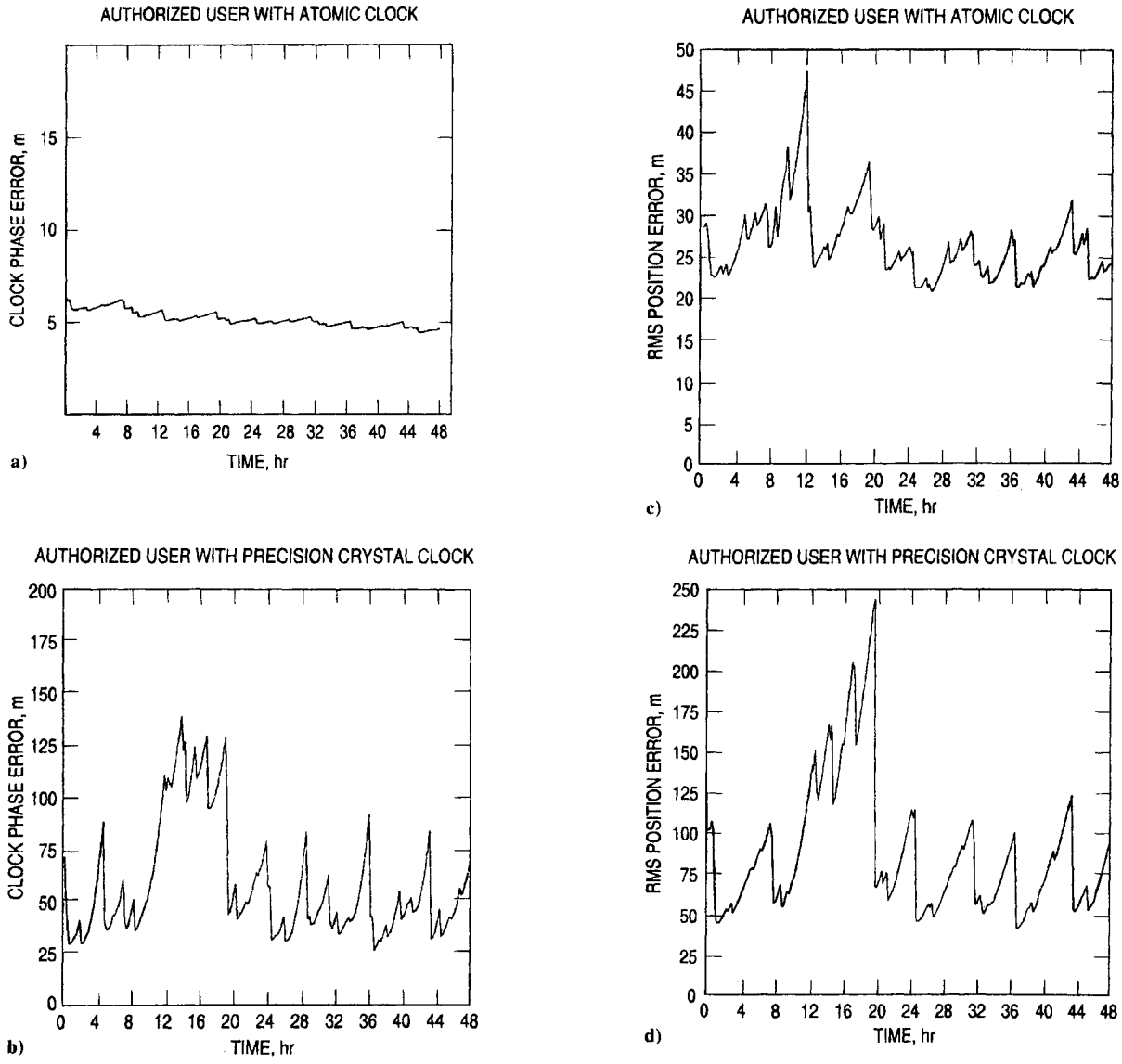

Fig. 3 Visibility, clock, and rms position curves.

4e and 4f show the ability of onboard determination in estimating the ΔV immediately after a stationkeeping maneuver. The 1σ error is 0.001 m/s using a crystal clock or 0.0005 m/s using an atomic clock. These ΔV estimation errors are one to two orders of magnitude smaller than the actual stationkeeping ΔV. The uncertainty of the thrusters may vary from 1 to 10% depending on spacecraft design. In this study, a conservative 15% (3σ) uncertainty is assumed for the thrusters.

Strategy A: Conventional Approach

This strategy is similar to the conventional longitude stationkeeping method being used by communication satellites with one midcourse correction between two successive ΔV maneuvers. The time of the midcourse correction will be 1 day after the nominal stationkeeping maneuver. The onboard sequential estimation can accurately determine the magnitude of the last ΔV and thus remove most of the thruster error with a second trim burn. The prediction of the time and size of the next stationkeeping maneuver can be accomplished either by predetermined values stored in the onboard processor or by a simplified algorithm explained in the Appendix.

A ± 0.1-deg longitude tolerance was assumed for the conventional approach. Longitude histories with onboard stationkeeping maneuvers were simulated for several values of initial longitudes using Program GEOSYN.[4] With a midcourse correction, the uncertainty of the maneuver can be effectively reduced from 15% (3σ) to 2.25% (3σ). Consequently, the longitude variation between two regular maneuvers follows closely the desired longitude history that occupies the entire tolerance band. The period of autonomy is a function of the rate of deviations from the desired longitude and the tolerance of the deviation.

Figure 6 shows how a midcourse ΔV can effectively remove a 15% undercorrection of a ΔV applied on day 33. In this case, the trim burn is performed 1 day after the regular maneuver, and the longitude histories reveal the 14-day variations due to lunar perturbations on geosynchronous orbit with high inclination ($i = 70$ deg).

For missions requiring inclination control, the previous strategy can be applied in the same procedure. However, the maneuver must be performed at the ascending or descending node rather than perigee or apogee. Furthermore, the prediction of inclination variation and stationkeeping ΔV should be made with an accurate ephemeris propagator on board the spacecraft.

Strategy B: Stationkeeping with Reduced Tolerance

This strategy is to reduce the current longitude tolerance to a smaller value or to a limit such that no midcourse ΔV is required to satisfy the accuracy requirement. The concept has some similarity with a semi-autonomous stationkeeping strategy previously reported.[5] For example, if the mean longitude of a geosynchronous satellite is controlled to within a reduced tolerance of 0.04 deg, the deviations from the desired mean longitude

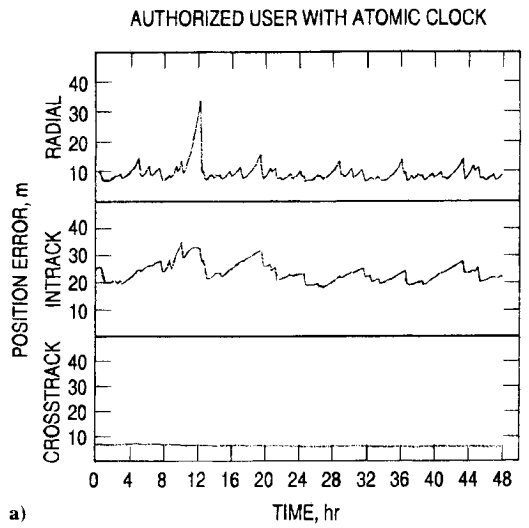

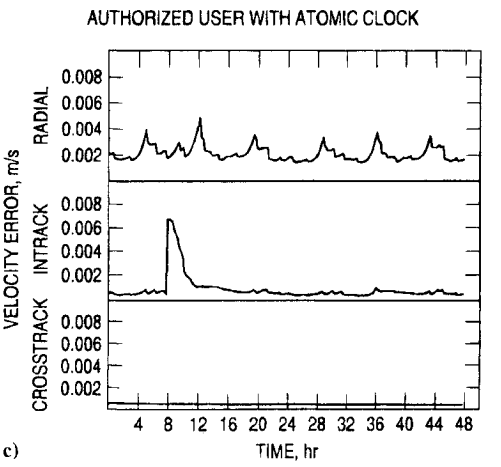

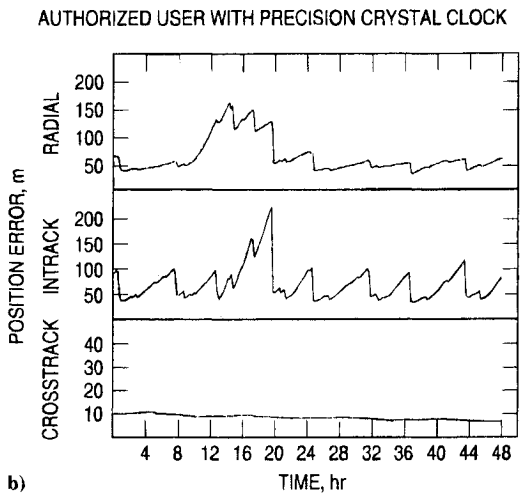

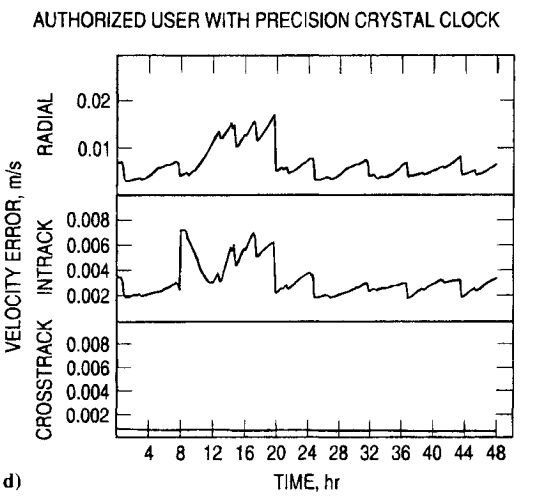

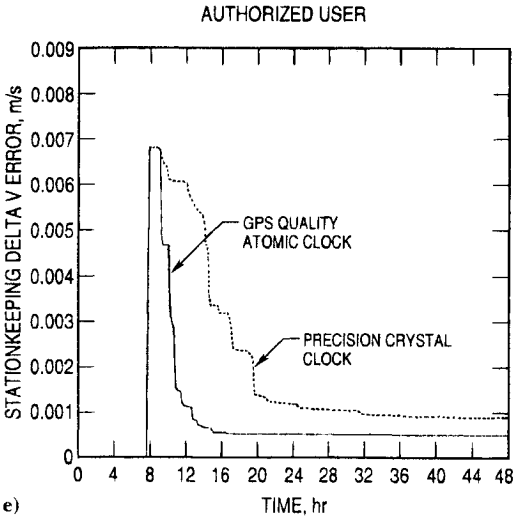

Fig. 4 Navigation component errors for authorized users.

will always be less than 0.04 deg. The time and magnitude of the next ΔV are estimated by the onboard GPS measurements through a sequential filter using the algorithm described in the Appendix. The advantage of the strategy is that the length of autonomy can be as long as the time that the onboard GPS receiver provides accurate measurements. This strategy can include the control of inclination as well. As a result, a geostationary satellite may be controlled to within a small box of about 0.04 deg in size without the need of ground support.

The longitude control tolerance is limited to thruster errors and the 14-day variations induced by lunar gravitational perturbations. For example, the amplitude of the 14-day variations is about 0.02 deg at 70 deg inclination as shown in Fig. 6. Thus, the longitude control tolerance must be increased from

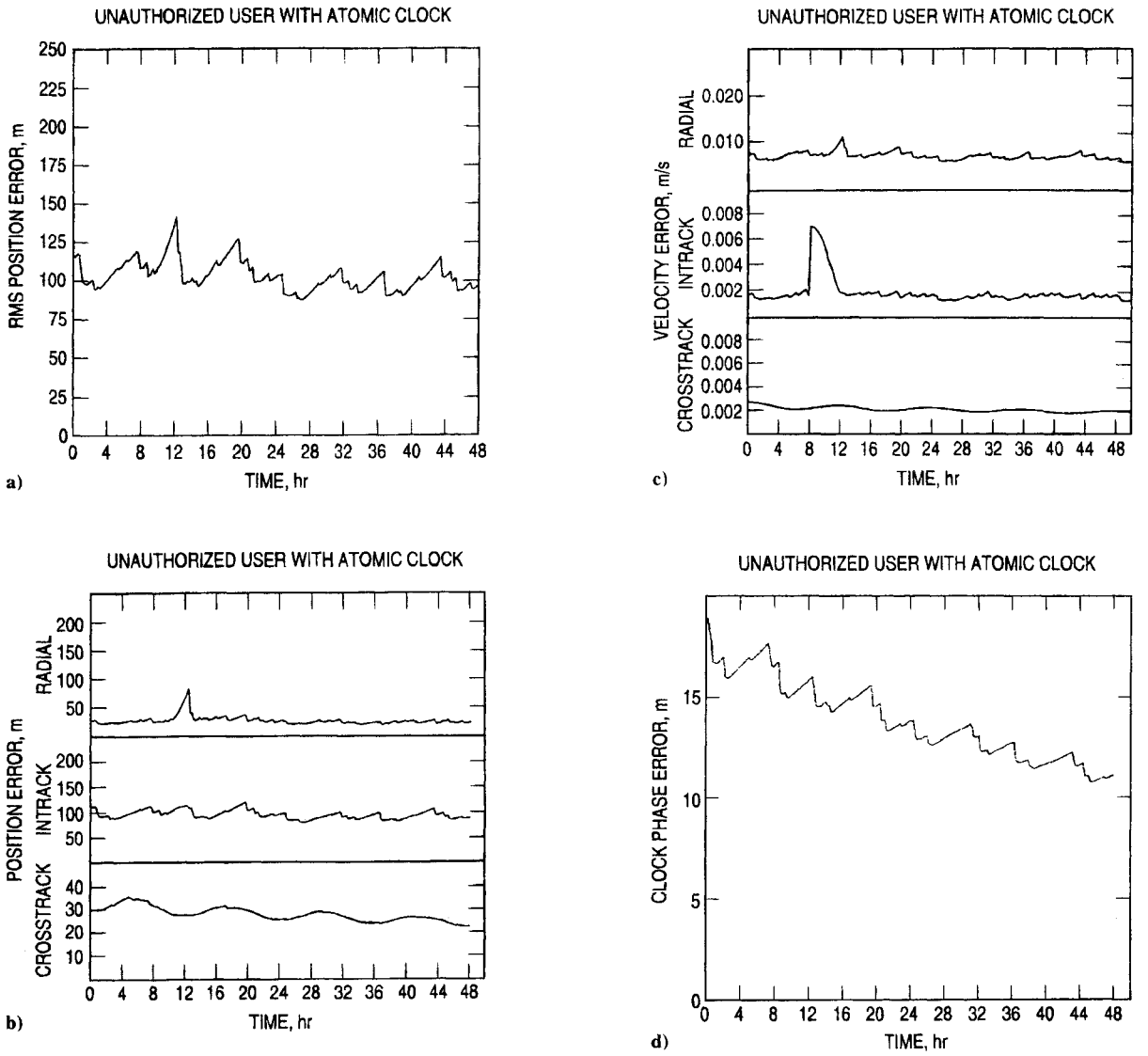

Fig. 5 Navigation component errors for unauthorized users.

Table 2 GPS onboard determination accuracy[a]

	Authorized user		Unauthorized user
	Crystal clock, position, m/velocity, m/s	Atomic clock, position, m/velocity, m/s	Atomic clock, position, m/velocity, m/s
In track	100/0.0025	25/0.0008	100/0.0017
Cross track	10/0.005	8/0.0005	28/0.0021
Radial	48/0.0055	12/0.0022	25/0.0065

[a]The numbers in this table are the average 1σ values obtained from Figs. 3, 4, and 8.

±0.04 to ±0.08 deg or larger to allow room for the 14-day variations. However, for geostationary orbits where the 14-day variations vanish, the longitude tolerance for autonomous stationkeeping can be further reduced with more accurate thrusters. Figure 7 shows the variations of longitude control time intervals as a function of longitude tolerance (in kilometers) and longitude of the satellite. As the tolerance of the mean longitude is reduced to ±2 km, the desired time interval between stationkeeping maneuvers varies from 5 days at 30°E to 11 days at 70°E, which is near the equilibrium point.

Note that a midcourse maneuver can also be used here 1 day after the regular maneuver to remove the thruster error. Then, the tolerance of longitude control may be further reduced to increase the accuracy of longitude prediction.

Strategy C: An Innovative Formation-Keeping Approach

The formation keeping of two nearby spacecraft with closed-loop feedback control algorithms has been studied and documented.[6-9] This concept is applied here to formation-keep a satellite with a fictitious spacecraft whose ephemeris is predetermined as the reference orbit. Taking advantage of the decoupling in the Clohessey-Wiltshire equations, the controllers for the in-plane and out-of-plane components are designed separately. The steady-state control laws are obtained by solving the discrete matrix Ricatti equation. This strategy requires at least three equally spaced small ΔV pulses within each orbit period to control the motion of the satellite according to the control laws.

The Clohessey-Wiltshire equations in a spacecraft-centered coordinate system are given next with x, y, and z being, respec-

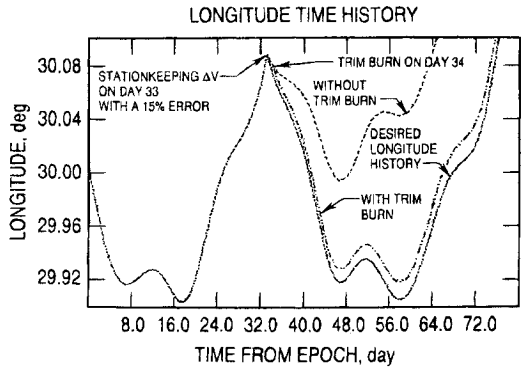

Fig. 6 Longitude diagram of onboard stationkeeping.

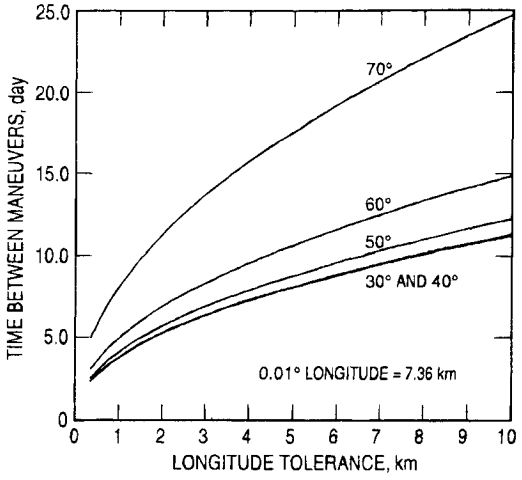

Fig. 7 Time between maneuver vs longitude tolerance.

tively, the in-track, cross-track, and radial deviations from a reference orbit:

$$\begin{aligned} \ddot{x} &= 2\omega_0 \dot{z} + f_x \\ \ddot{y} &= -\omega_0^2 y + f_y \\ \ddot{z} &= -2\omega_0 \dot{x} + 3\omega_0^2 z + f_z \end{aligned} \tag{1}$$

where ω_0 is the orbit mean motion, and f_x, f_y, and f_z are the three components of the unmodeled spacecraft accelerations, such as the uncertainties of the Earth gravity harmonics and solar radiation pressure model. The cost functions for in-plane and out-of-plane components are

$$\begin{aligned} J_1 &= \frac{1}{2}\sum_{k=1}^{\infty}\left[x_k^2 + \left(\frac{\Delta V_{xk}}{\omega_0}\right)^2 + \left(\frac{\Delta V_{zk}}{\omega_0}\right)^2\right] \\ J_2 &= \frac{1}{2}\sum_{k=1}^{\infty}\left[x_k^2 + \left(\frac{\Delta V_{yk}}{\omega_0}\right)^2\right] \end{aligned} \tag{2}$$

where J_1 is the cost function for in-plane components, and J_2 is the cost function for out-of-plane components. The variables x_k and y_k are the in-track and cross-track deviations at time k, respectively; and ΔV_{xk}, ΔV_{yk}, and ΔV_{zk} are the small velocity changes at time k along in-track, cross-track, and radial directions.

The discrete state equations are as follows:

Out of plane:

$$\begin{bmatrix} \dot{y}_k + 1 \\ y_k + 1 \end{bmatrix} = [C]\begin{bmatrix} \dot{y}_k \\ y_k \end{bmatrix} + [D][\Delta V_{yk}] \tag{3a}$$

In plane:

$$\begin{bmatrix} \dot{x}_k + 1 \\ x_k + 1 \\ \dot{z}_k + 1 \\ z_k + 1 \end{bmatrix} = [A]\begin{bmatrix} \dot{x}_k \\ x_k \\ \dot{z}_k \\ z_k \end{bmatrix} + [B]\begin{bmatrix} \Delta V_{xk} \\ \Delta V_{zk} \end{bmatrix} \tag{3b}$$

where matrices A, B, C, and D are the transition matrices obtained from two-body solutions. The steady-state control laws are obtained by solving the discrete matrix Ricatti equation for two maneuver frequencies, three times and four times per revolution. The results of the control equations are for in-plane motion at Δt = 8 h = interval between thrusts

$$\begin{bmatrix} \Delta V_{xk} \\ \Delta V_{zk} \end{bmatrix} = \begin{bmatrix} -0.9354 & 0.0100 & 0.0814 & 1.6303 \\ 0.0814 & -0.2763 & -0.8138 & -0.8401 \end{bmatrix} \begin{bmatrix} \dot{x}_k \\ \omega_0 x_k \\ \dot{z}_k \\ \omega_0 z_k \end{bmatrix} \tag{4}$$

and at Δt = 6 h

$$\begin{bmatrix} \Delta V_{xk} \\ \Delta V_{zk} \end{bmatrix} = \begin{bmatrix} -0.8917 & 0.0439 & 0.1096 & 1.4793 \\ 0.1096 & -0.3668 & -0.7834 & -1.0091 \end{bmatrix} \begin{bmatrix} \dot{x}_k \\ \omega_0 x_k \\ \dot{z}_k \\ \omega_0 z_k \end{bmatrix} \tag{5}$$

and for out-of-plane motion at Δt = 8 h

$$\Delta V_{yk} = -0.6073\,\dot{y}_k + 0.1549\,\omega_0 y_k \tag{6}$$

and at Δt = 6 h

$$\Delta V_{yk} = -0.6180\,\dot{y}_k + 0.0012\,\omega_0 y_k \tag{7}$$

Three cases of GPS onboard determination accuracy are assumed in this study. The navigation errors (1σ) associated with an authorized user with a crystal and an atomic clock and an unauthorized user with an atomic clock are shown in Table 2. A series of simulations was generated for two thrusting frequencies, once every 8 and 6 h based on the assumed statistics. A 15% (3σ) error is assumed along each of the three directions of impulsive burns. Figure 8 shows how rapidly the

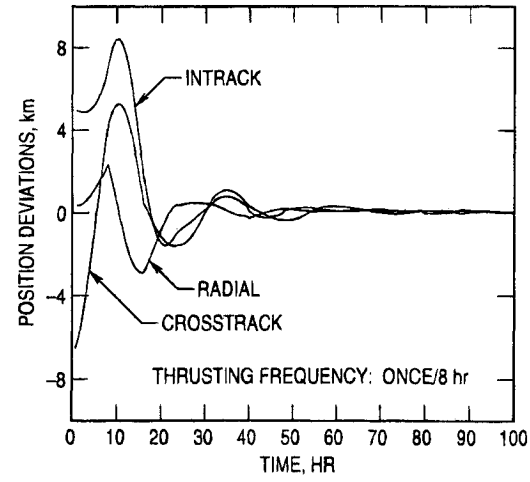

Fig. 8 Deviation with feedback control starting from large initial position deviation.

position deviations are reduced to within a fraction of a kilometer after 40 h of small orbit control maneuvers (once every 8 h). Figures 9–11 are examples of the histories of deviations along the radial, in-track, and cross-track directions for a period of 480 h with feedback control. The errors in GPS navigation are simulated by random number generators (1σ noise with 0 mean). The simulation results are summarized in Table 3. The maximum deviations from the predetermined reference trajectory depend strongly on the onboard clock performance and whether it is an authorized user. For authorized user satellites with an atomic clock, the maximum deviations are very small, 80 m for an 8-h thrusting frequency and 65 m for a 6-h thrusting

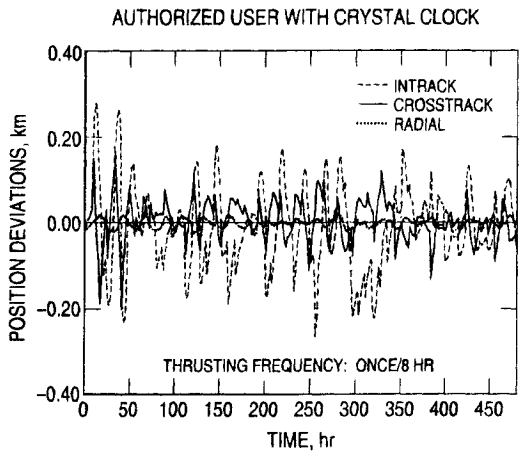

Fig. 9 Deviations with feedback control, example 1.

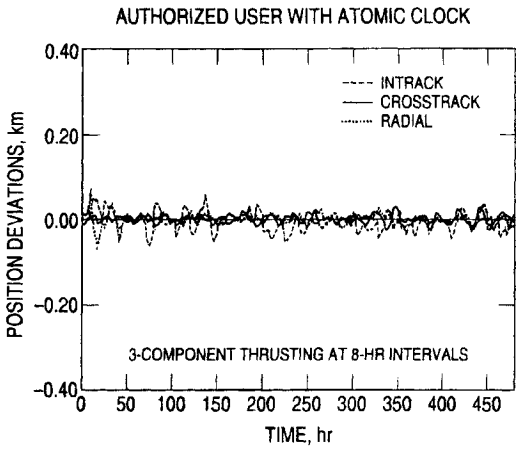

Fig. 10 Deviations with feedback control, example 2.

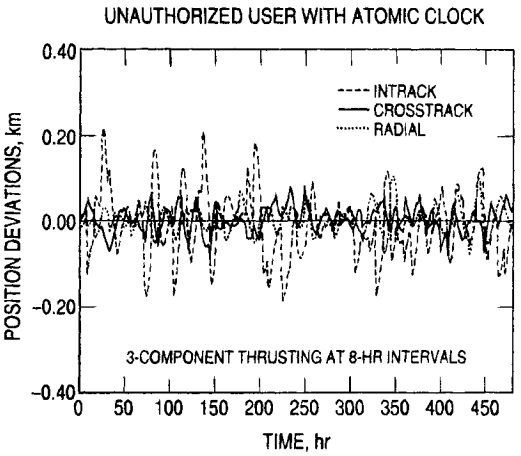

Fig. 11 Deviations with feedback control, example 3.

frequency. However, the maximum deviations become three to four times greater when either a crystal clock is used or the user satellite is unauthorized. Table 3 also shows the ΔV requirements for the orbit control maneuvers. It is interesting to note that the ΔV requirements of an authorized user with a crystal clock are about three times more than the same satellite with an atomic clock. This is because most of the ΔV is needed to correct the error in the GPS measurements, which are driven by the clock performance. The maximum deviations and ΔV requirements associated with an unauthorized user are similar to that of an authorized user with a crystal clock as shown in Table 3. The case of an unauthorized user with a crystal clock is not considered here because the ΔV requirements may be too large to be acceptable. The case with an 8-h thrusting rate and an atomic clock requires the least amount of ΔV (2.5 m/s).

From an orbital mechanics point of view, the in-track variations are correlated with the radial variations, and thus the ΔV along the radial direction may be eliminated to reduce the ΔV expenditure. The control law then becomes for an 8-h thrusting rate

$$\Delta V_{xk} = [-0.9940 \quad 0.0775 \quad 0.2776 \quad 1.8931] \begin{bmatrix} \dot{x}_k \\ x_k \\ \dot{z}_k \\ z_k \end{bmatrix}$$

and for a 6-h thrusting rate

$$\Delta V_{xk} = [-0.9873 \quad 0.1129 \quad 0.4513 \quad 1.9858] \begin{bmatrix} \dot{x}_k \\ x_k \\ \dot{z}_k \\ z_k \end{bmatrix}$$

The same simulations were repeated with the previous control laws without thrusting along the radial direction. Results (Table 3) indicate that the ΔV requirements can be reduced by 20–40% depending on the type of clock, for the case with one per 8-h thrusting rate. However, the corresponding maximum position deviations increase to 220 m using an atomic clock and to 700 m using a crystal clock. For missions with a tight budget on propellant weight, such a tradeoff is justified.

The previous three stationkeeping strategies using a GPS receiver reveal the potential of significantly reducing ground support in the routine maintenance of geosynchronous satellites. The unique capability of highly accurate, long-term ephemeris prediction inherent in the formation-keeping approach offers important applications for future space missions.

Conclusions

A detailed description of the feasibility and inherent accuracy of onboard orbit control of a geosynchronous satellite using a GPS receiver has been provided. The additional fuel required to accurately control the satellite motion to a predetermined ephemeris is small. The contributions of this technique to the space community are twofold. First, accurate, long-term satellite ephemeris predictions become routine and reliable with accuracies currently not achievable. As a result, the predetermined satellite ephemeris can be distributed to the users several months in advance with assured accuracy. Second, the potential to largely eliminate ground support means significant cost savings.

Although this analysis is restricted to geosynchronous satellites, the technique can be applied to other missions with near-circular orbits. In the case of orbits with altitudes lower than that of GPS, the accuracy of orbit control would improve due to the favorable visibility to GPS satellites. The important potential contributions of this innovative technique also encourage the study of extending its application to orbits with moderate and large eccentricity.

Table 3 Maximum deviations of ΔV requirements for orbit control

Thrusting frequency, h	Thrusting components[a]	Authorized user: Maximum deviation[b], m	Authorized user: ΔV requirement/yr[b], m/s	Unauthorized user: Maximum deviation, m	Unauthorized user: ΔV requirement/yr, m/s
6	3	65/260	5.5/13.9	260	12.9
8	3	80/270	4.4/11.8	280	9.8
6	2	200/670	4.2/11.7	350	10.2
8	2	220/700	2.5/7.3	510	6.8

[a]Three components: radial, in track, and cross track; two components: in track and cross track.
[b]Values associated with atomic clock/values associated with crystal clock.

Appendix: Algorithm for Strategy A

Stationkeeping methods for geostationary satellites have been studied during the past two decades.[10-12] The derivation of the equations for long-term longitude variations can be found in Refs. 10 and 11. This section describes a very efficient algorithm for determining stationkeeping ΔV and the time of maneuver. This is a useful algorithm for the onboard autonomous stationkeeping strategies.

For a tight longitude tolerance of ± 0.1 deg or less, a good approximation is that the longitude variations within the narrowband can be represented by the following expression:

$$\frac{d^2\lambda}{dt^2} = \epsilon \tag{A1}$$

Integrate once to give the longitude drift equation

$$\frac{d\lambda}{dt} = \dot{\lambda}_0 + \epsilon t \tag{A2}$$

Integrate twice to give the longitude deviation from an initial value at $t = 0$

$$\delta\lambda = \dot{\lambda}_0 t + \frac{\epsilon}{2} t^2 \tag{A3}$$

Apply the conditions of an optimum stationkeeping:

$$\frac{d\lambda}{dt} = 0 \tag{A4a}$$

and at $t = t_m$

$$\delta\lambda = \delta\lambda_b \tag{A4b}$$

where t_m is the midpoint of the time interval between two successive stationkeeping maneuvers, and $\delta\lambda_b$ is the maximum deviation that occurs at t_m. Then the two equations can be obtained after eliminating $\dot{\lambda}_0$. The combined equations can be used to solve for the time of the next stationkeeping maneuver, and then the ΔV can be determined. However, in practice, the solutions do not always give satisfactory predictions of ΔV due to the influence of other perturbations such as luni-solar attractions. A small correction term to account for the slow variation in ϵ is added to the equation as follows:

$$\delta\lambda_b = -\frac{\epsilon}{2} t_m^2 - \frac{\dot{\epsilon}}{3} t_m^3 \tag{A5}$$

Solve for t_m by iteration,

$$t_m = \sqrt{\frac{-2\delta\lambda_b}{[\epsilon + (2/3)\dot{\epsilon} t_m]}} \tag{A6}$$

The two small constants ϵ and $\dot{\epsilon}$ can be determined either analytically from tesseral harmonics (J_{22}) and luni-solar perturbation equations or numerically from longitude variations.

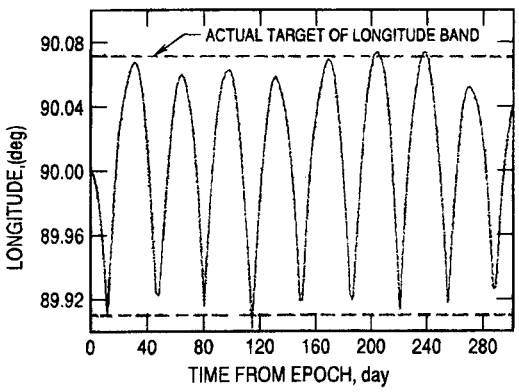

Fig. A1 Longitude time history of geosynchronous satellite with stationkeeping.

Based on previous experience in using program GEOSYN[2], this algorithm has been found to be very effective and accurate when using the numerical approach. For symmetrical longitude variations before and after a maneuver, the ΔV can be determined with an accuracy around 5% with the following equation:

$$\Delta V = (2/3)a[\epsilon t_m + (\dot{\epsilon}/2)t_m^2] \tag{A7}$$

where a is the orbit semimajor axis.

For nonsymmetrical longitude variations,

$$\Delta V = \tfrac{1}{3}\, a[e(t_m + t_m') + (\epsilon/2)(t_m^2 + t_m'^2)] \tag{A8}$$

where t_m' is the midpoint time of the previous stationkeeping interval where the maximum deviation is different than the current value of $\delta\lambda_b$. Figure A1 shows an example of longitude time history with stationkeeping using this algorithm. The well-behaved variations indicate the accuracy of the previous method.

Acknowledgments

This work reflects research conducted under U.S. Air Force Space Systems Division Contract F04701-88-C-0089. The authors are grateful to W. H. Boyce and R. J. Perkins for their initial support of this study. The authors would like to thank S. Sokolsky, W. A. Feess, and R. G. Hopkins of The Aerospace Corporation for their efforts in reviewing this paper. Thanks are due to C. B. Dunbar for solving the discrete matrix Ricatti equations using the MATLAB on a VAX computer.

References

[1] Ananda, M. P., and Jorgensen, P. S., "Orbit Determination of Geostationary Satellites Using the Global Positioning System," *Proceedings of Symposium on Space Dynamics for Geostationary Satellites*, Centre National d'Etudes Spatiales, Toulouse, France, Aug. 1985.

[2] Wu, S. C., Yunck, T. P., Lichten, S. M., Haines, B. J., and Malla, R. D., "GPS-Based Precise Tracking of Earth Satellite from Very Low to Geosynchronous Orbits," National Telesystems Conference, George Washington Univ., Washington, DC, May 19–20, 1992, pp. 4-1–4-8.

[3] Malys, S., and Holm, S., "PPS and SPS Integrity Monitoring with an Independent Global Tracking Network," *Proceedings of the Institute of Navigation GPS-92*, Fifth International Technical Meeting of the Inst. of Navigation, Albuquerque, NM, Sept. 16–18, 1992, pp. 979–984.

[4] Chao, C. C., and Baker, J. M., "On the Propagation and Control of Geosynchronous Orbits," *Journal of Astronautical Science*, Vol. 31, No. 1, 1983, pp. 99–115.

[5] Chao, C. C., "Semiautonomous Stationkeeping of Geosynchronous Satellites," *Journal of Guidance, Control, and Dynamics*, Vol. 7, No. 1, 1984, pp. 57–61.

[6] Vassar, R. H., and Sherwood, R. B., "Formationkeeping for a Pair of Satellites in a Circular Orbit," *Journal of Guidance, Control, and Dynamics*, Vol. 8, No. 2, 1985, pp. 235–242.

[7] Hubert, S., and Swale, J., "Stationkeeping of a Constellation of Geostationary Communications Satellites," AIAA Paper 84-2042, Aug. 1984.

[8] Swinerd, G. G., and Murdoch, J., "An Assessment of Satellite-to-Satellite Tracking Applied to Satellite Clusters," AAS/AIAA Astrodynamics Conference, AAS Paper 85–387, Vail, CO, Aug. 1985.

[9] Leonard, C. L., "Fuel Penalty of Using Ballistic Coefficient Control for Satellite Formationkeeping," AAS 13th Annual Guidance and Control Conference, Keystone, CO, Feb. 1990.

[10] Michielsen, H. F., and Webb, E. D., "Stationkeeping of Stationary Satellites Made Simple," *Proceedings of the First Western Space Conference*, 1970, pp. 704–727.

[11] Kamel, A., Ekman, D., and Tibbitts, R., "East-West Stationkeeping Requirements of Nearly Synchronous Satellites Due to Earth's Triaxiality and Luni-Solar Effects," *Celestial Mechanics*, Vol. 8, 1973, pp. 129–148.

[12] Lovell, R. R., and O'Malley, T. A., "Stationkeeping of High Power Communication Satellites," NASA-TM-X-2136, Nov. 1970.